ORIGINAL ARTICLE

Metallographic behavior in the fracture of a pendant of an endless screw conveyor

Comportamiento metalográfico en la fractura de un colgante de transportador de tornillo sinfín

Lisander Romero-Breffe[1], Daniela García-Torres[1]

[1]University Moa, Holguín, Cuba.

*Corresponding author: lromerob@ismm.edu.cu

Abstract

This study aims to determine the internal structure in the fracture failure of pendant of an endless screw conveyor made of AISI 4340 steel. The fractured element was visually inspected and cut into sections, close to the damaged area and the furthest from it for determining the hardness effect after the event occurred. The methodology to establish the percentage of microconstituent was established. Our results showed that the fracture failure of pendant is caused by the forming concentric circular marks with beach marks on fatigue fracture, indicating fracture by cleavage mechanism, where hardness values in the fracture zone are between 329.8 HV and in the zone farther away from the failure, the value is 326.4 HV, property reached when applying tempering heat treatment at 600 °C.

Keywords: pendant, fracture, fatigue, cracks, internal structure, screw conveyor

Resumen

La investigación se enfoca en determinar la estructura interna en la falla por fractura de un colgante de un transportador de tornillo sinfín fabricado de acero AISI 4340. Se realizó la inspección visual al elemento fracturado, el cual fue cortado en secciones, próximo al área fracturada y en la más alejada de ella para determinar el efecto de la dureza luego de ocurrido el fenómeno. Se estableció la metodología para establecer el porcentaje de microconstituyentes. Se determina que la falla por fractura del colgante es ocasionada por la formación de marcas circulares concéntricas con marcas de playa en fractura por fatiga, indicativo de fractura por mecanismo de clivaje, donde los valores de dureza en la zona de fractura se encuentran entre los 329,8 HV y en la zona más alejada de la falla, el valor es de 326,4 HV; propiedad que se alcanza al aplicar tratamiento térmico de revenido a 600°C.

Palabras claves: colgante, fractura, fatiga, grietas, estructura interna, transportador de tornillo sinfín

1. INTRODUCTION

Fatigue is a form of fracture that occurs in metal structures subjected to variable stresses. The term "fatigue" is used because this type of fracture occurs after a period of cyclic stresses, which arise from the effect of repetitive loads. August Wöhler introduced the S-N curves (stress-number of cycles) that bear his name to describe the relationship between the amplitude of cyclic stresses and the number of cycles to failure. The applied cyclic stresses can be axial, flexural, or torsional in nature (Cavalieri *et al*., 2011; Gainza-Legrá, 2016).

Fatigue fracture begins with small cracks that grow under the action of fluctuating stress. It is characterized by a maximum value lower than the tensile strength. Under the action of low-level repetitive load applications, the crystal structure of the metal can undergo changes leading to the formation of small and large cracks, provided the cyclic loading continues, which can eventually lead to the fracture of the part. Once this type of failure is initiated, it can propagate at high stresses and low cycles or at low stresses and high cycles. It may exhibit different characteristics, resembling brittle or ductile fracture, depending on the type of material involved, stress circumstances, or environmental causes (Vázquez *et al*., 2023; Megias *et al*., 2023).

The fatigue properties of materials are determined from laboratory tests. These tests must, as far as possible, accurately reproduce the service conditions of the material. Traditionally, the material is subjected to relatively high cyclic stresses, and the number of cycles to failure is recorded; the amplitude of the maximum stresses is then reduced, and the experiment is repeated. It is important to mention that the number of cycles is associated with the life of the material; that is, the useful life of a structure can be guaranteed if the stresses are maintained at a fixed value (Govindu & Jayananh, 2015; Inzana *et al*., 2016).

Loads whose amplitudes vary over time produce failure in structures at stress values lower than those occurring in cases of constant amplitude loads. This phenomenon is what we term fatigue. It is generally defined by ASTM standards as "the process of progressive localized permanent structural change occurring in a material subjected to conditions that produce fluctuating stresses and strains at some point or points and that may culminate in cracks or complete fracture after a sufficient number of fluctuations" (Jaramillo & Bacca, 2009; Lee *et al*., 2014).

Furthermore, fatigue fracture theory allows for the prediction of crack growth with load cycles. Therefore, traditional calculation methods, together with fatigue fracture theory, provide a solid basis for the design of metal structural systems (Madenci & Guven, 2015).

The objective of this work is to determine the metallographic behavior in the fracture of a pendant of an endless screw conveyor.

2. MATERIALS AND METHODS

Table 1 shows the chemical composition of AISI 4340 steel, according to the Alloy Casting Institute (ACI), AISI - SAE, the American Society for Testing and Materials (ASTM), and SAE.

Table 1. Chemical composition of AISI 4340 steel; % by mass

Grade	C	Mn	P	S	Si	Ni	Cr	Mo	Fe
AISI 4340	0.38-0.43	0.75-1	< 0.035	< 0.04	0.15-0.35	< 0.25	0.8-1.1	0.20-0.30	Balance

AISI 4340 steel is a low-alloy steel, as it contains less than 10% alloying elements per the AISI standard (43XX). The main elements are nickel, chromium, and molybdenum, which impart different properties to the material, such as corrosion resistance (Cr), increased hardenability and toughness (Ni), and increased hot strength and creep resistance (Mo) (Albarbar, 2013; Ayatollahi *et al*., 2014).

2.1. Metallographic preparation of specimens

The model in Figure 1 was considered for the metallographic analysis of the pendant belonging to the trough of a screw conveyor.

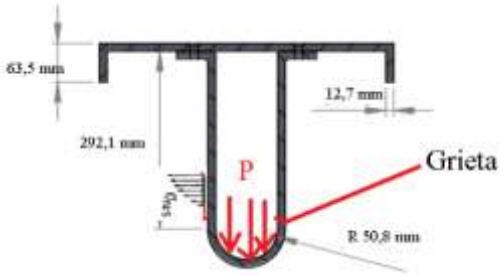

Figure 1. Load conditions.

The residual stress distribution is a type of load produced by stresses generated during the rolling process. Since the material is assumed to be linear-elastic, the principle of superposition will be applicable and used to account for the residual stress distribution in the pendant.

Prior to the visual inspection, the piece was cleaned to remove the covering of grease or dust, which was entirely removed with thinner and a soft-bristle brush. As shown in Figure 2, concentric circular marks are observed on the pendant.

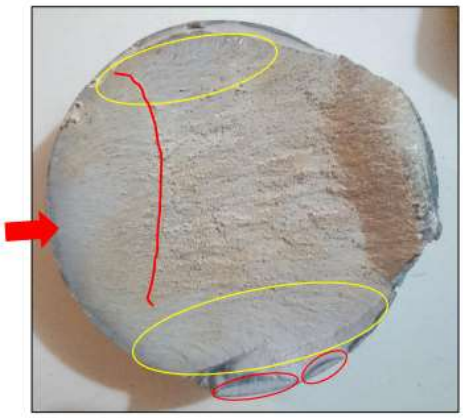

Figure 2. Fracture mechanism of AISI 4340 steel.

In the fracture mechanism, the initiation of the crack indicated by the arrow is observed, as well as beach marks in the area highlighted with a yellow circle; the boundary or change in the material marks is highlighted by a red line. Subsequent to this line in the direction of the arrow, a change in morphology appears, with another type of fracture being observed as if it had been torn, as well as numerous marks of a brittle fracture, indicated by red circles, due to the martensite on the material surface.

For the preparation of the specimens, a set of operations was performed on the sample, such as: selection, extraction or cutting, mounting and preparation, etching, microscopic analysis, and obtaining photomicrographs (NC 10 - 56:86 and ASTM E 3 – 95).

When selecting the part to be studied, care was taken to ensuring that it had not been affected by another previously executed process. The size of the specimen was chosen such that it could be held by hand during its preparation and depending on the working area of the chosen microscope. Samples of the pendant employed in the production process were selected.

2.2. Cutting of samples

The cutting machine used for the preparation of the specimens is a CM 260 type, echo RD brand. It possesses five jets of coolant liquid that ensure constant lubrication to avoid heating and, consequently, microstructural transformations on the contact surfaces. Figure 3 shows the cutting area of the specimens.

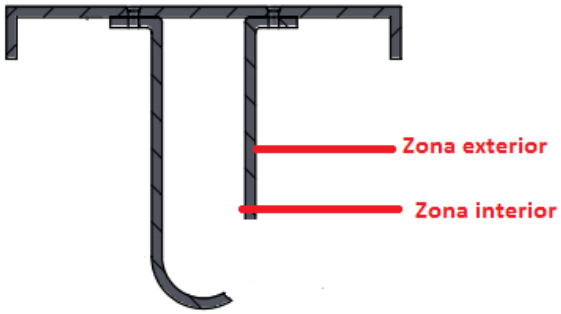

Figure 3. Cutting area of the specimens.

The cutting was performed in such a way that the microstructure could be observed according to the geometric configuration; enabling, in addition, its easy handling and subsequent leveling, as well as chemical etching. Three specimens were considered and encapsulated with ROYAPOX 50-50 epoxy resin to perform the grinding and polishing operations and ensure ease of handling. The operation was carried out with an echo RD brand machine, type MP 350 A.

To perform microstructural analysis on the edges of deformed samples, it is important to maintain a 90º angle throughout the observation area, since, during grinding and polishing operations, these edges become distorted and rounded, resulting in a false observation of the image under the microscope.

2.3. Grinding and polishing operation

This was carried out by varying the granulometry of the abrasive papers applied to the workpiece, from coarsest to finest, types No. 400, 600, and 800 (ASTM E 3-95). The sandpapers were placed on a glass plate (Figure 4). The sanding direction was changed by 90º when passing from one grit to another to eliminate the layer of distorted and slipped material left by the previous one; this allowed for obtaining a smooth and polished surface, free of impurities or scratches. Finally, the samples were polished on a MONTASUPAL brand metallographic polisher.

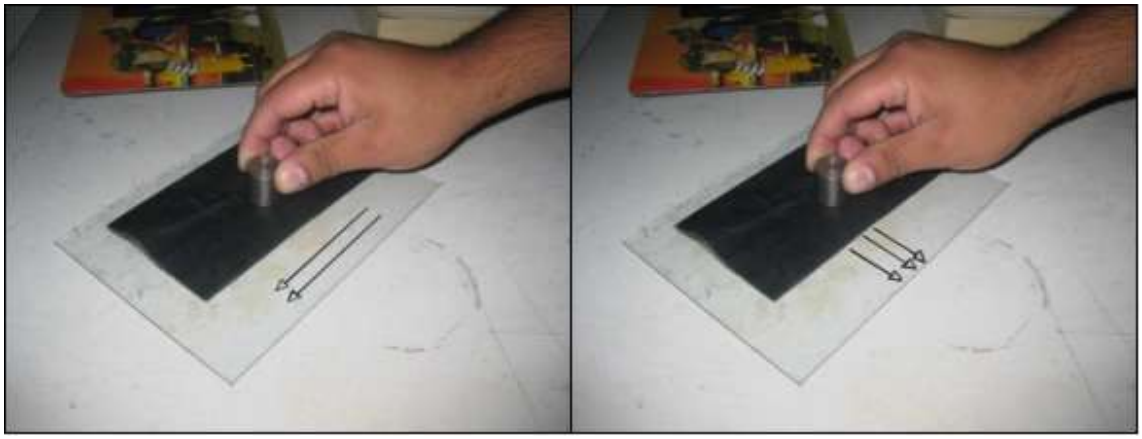

Figure 4. Grinding of the specimens.

To etch the specimens, 5% Nital was used as a chemical reagent. It was poured into a capsule into which the specimen was introduced; the etching was stopped by submerging the specimens in water, and then the surface was observed. After etching, the specimen was washed again with abundant running water, dried with alcohol (absolute), and air-dried.

2.4. Microstructural behavior

The specimens were observed under a NOVEL brand binocular optical microscope, model NIM–100. This is equipped with a camera installed via IMI.VIDEOCAPTURE.exe hardware that reflects the photograph on the computer. Once the lens height was regulated, a 640 x 480-megapixel photomicrograph was obtained through Scope Photo software, as shown in Figure 5.

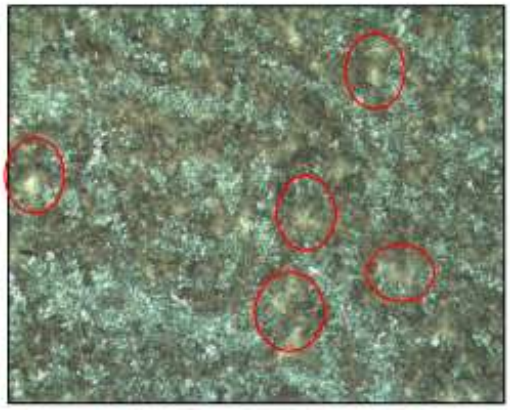

Figure 5. Metallography of AISI 4340.

The microstructure is consistent with the presence of bainite with some retained austenite indicated by the circles; basically, it is a microstructure expected for this type of material due to the nickel percentages.

To place the specimens in the microscope and avoid distorted observation of the images, they were placed in a device with plasticine, which allowed for parallel leveling with respect to the observation objective. The microstructural analysis consisted of observing a sample of AISI 4340 steel. The objective of this analysis was to obtain a sample unaffected in its crystal structure that would allow determining the heat treatment to which the hopper was exposed before being put into operation.

2.5. Determination of microconstituents

For this purpose, an echoLAB brand reflective binocular optical microscope was used, equipped with a camera installed via hardware that projects the photograph onto the computer. It performs light reflection from the polished specimen with an attached digital camera, which connects from the microscope to a LENOVO laptop, containing an image analyzer program for images taken from the camera.

Phases, grain size, inclusions, and grain affectations were evaluated, and a technical report with these characteristics was prepared. In this test, the grains will present different colors; additionally, atoms at the boundaries are more reactive during chemical etching and dissolve in greater quantity than the grain itself, thus reflectivity changes and visibility is enhanced. The stages considered for digital image processing are constant for different software, and their application depends on the desired product.

The procedure for the analysis of microconstituents according to ASTM A 247 standard is shown in Table 2.

Table 2. Procedure for the analysis of microconstituents

Microconstituents	Area	Area %
1	Area 1	Area 1
2	Area 2	Area 2
3	Area 3	Area 3

The procedure was necessary to estimate the percentages of microconstituents present in the different zones analyzed in the hopper, with which, in turn, the hardness in this zone can be estimated. In this test, when grains in the structure present different colors, it indicates the existence of more than one microconstituent.

2.6. Microhardness test applied to samples

The microhardness test was performed to determine the hardness of microscopically small volumes in the alloy. An HTU 200 BVR D model microscope was used. The applied load was 0.49 N, for a time of 15 s. The indenter used was a diamond pyramid, with an angle of 136º according to ASTM E 92-82.

3. ANALYSIS OF RESULTS

3.1. Chemical composition of AISI 4340 steel

Table 3 shows the chemical composition of AISI 4340 steel determined in a SPECTROLAB 230 quantum mass spectrometer, with a carbon electrode under submerged arc in an argon atmosphere.

Table 3. Chemical composition of AISI 4340, % by mass

Grade	C	Mn	P	S	Si	Ni	Cr	Mo	Fe
AISI 4340	0.396	0.746	0.035	0.04	0.262	1.771	0.81	0.25	Balance

3.2. Microstructural behavior of the pendant

The microstructural behavior of the AISI 4340 steel was analyzed subsequent to the fracture phenomenon, considering the microstructure of the material in the as-delivered state. Figure 6 shows a heterogeneous microstructure of bainite, tempered martensite, and islands of untempered martensite; the presence of a ferrite zone and non-metallic manganese sulfide (MnS) inclusions is also appreciated.

The addition of manganese (Mn) in steels is due to its greater affinity than iron to combine with sulfur and form manganese sulfide, which thus prevents the undesirable formation of iron sulfide, which has a low melting point and produces internal fissures when the steel is hot rolled.

The structure presents upper bainite rods and ferrite grains in lower proportion. This is the product of air cooling (normalizing) from a temperature higher than the austenitizing temperature, which occurred after rolling. No significant differences are observed between the structures in the cross-section to the rolling direction, and this is because total recrystallization of the austenitic grains occurred after plastic deformation.

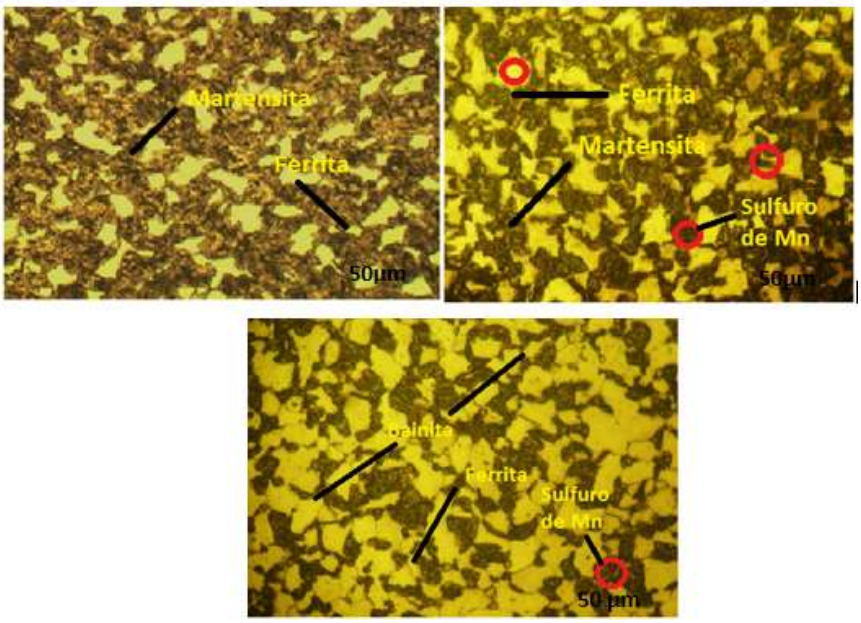

Figure 6. Microstructure of AISI 4340.

The observed microstructural heterogeneity is a consequence of chemical diversity in the material, which presents quenching and tempering heat treatments. In steels with more than 0.4% C, when quenched to room temperature, decomposition of retained austenite occurs caused by tempering at temperatures between 200 °C and 300 °C, transforming it into bainite. This explains the increase in hardness in high-carbon steels for low-temperature tempering, as bainite is harder than austenite. Above 350 °C, the loss of hardness is caused by a recrystallization effect, as reported by Srivastava *et al*. (2015).

The fracture of the AISI 4340 steel, belonging to the trough of the screw conveyor, may be originated by one-step embrittlement, a mechanism that could be caused by impurities in the steel. This phenomenon affects low-alloy steels quenched to martensite and then tempered in the range of 250 °C to 350 °C. It is characterized by hardness decreasing continuously, while impact resistance passes through a minimum, exactly at 350 °C, and then rises. Furthermore, embrittlement is accompanied by predominantly intergranular fracture. Alloying elements such as manganese can have an indirect effect on promoting the segregation of embrittlement elements at grain boundaries, a criterion that coincides with Mantwatkar and Chavan (2016); Guerra-Fernández *et al*. (2019).

3.3. Phases present in the steel

The analysis of the distribution of microconstituents in the structure allowed determining the influence exerted by the phase on the fracture phenomenon

of AISI 4340 steel. Figure 7a corresponds to the microstructure of the steel and 7b to the microconstituents belonging to this distribution.

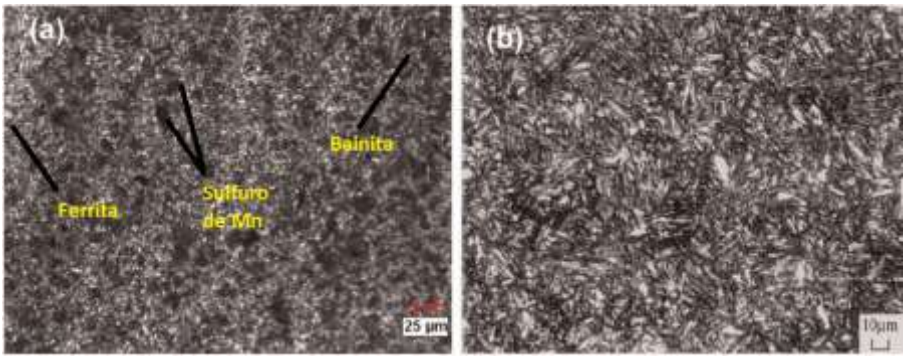

Figure 7. a) Microstructure AISI 4340 b) Microconstituents.

In the distribution of microconstituents or phases (Figure 7b), a heterogeneous distribution of these over the structure is observed. On the other hand, no significant differences are observed between the structures in the cross-section to the rolling direction, due to the total recrystallization of austenitic grains after plastic deformation. A distribution of bainite and ferrite grains in the form of rods is distinguished; this behavior is the product of air cooling (normalizing) from a temperature higher than the austenitizing temperature, which occurred after rolling.

Table 4 shows the distribution of phases on the structure and the area they occupy on it. The microstructure in the core of the pendant of the screw conveyor trough is composed of martensite (51.24%), followed by ferrite with an area of 21.6% and bainite with 26.96%, a structure that tends to present larger grains and, consequently, a reduction in hardness. In the lower part where the failure occurred, presumably this distribution caused tearing in the direction of force application due to the effect of the ferritic phase.

Table 4. Data of present phases

Microconstituents	Area	Area %
Martensite	345 274	51.24
Ferrite	306 783	21.6
Bainite	167 671	26.96

3.4. Hardness behavior in the pendant

Vickers hardness (HV) must be considered as a plastic hardness, since it has been determined from the permanent or residual indentation, that is, on the

plastic deformation obtained on the material surface after penetration. Table 5 reports the hardness results obtained for the material according to each sample selection condition. A scheme of the hardness measurement sequence in the transverse and longitudinal sections of the samples is shown.

Table 5. Hardness behavior

Sample	Fracture Zone (HV avg)	Zone Distal from Fracture (HV avg)
1	329.8	325.9
2	330.4	326.4
3	331.1	327.0

The hardness values for the sample measured in the fracture zone are approximately between 329.8 HV (32.3 HRC), and in the zone furthest from the failure, the value is 326.4 HV (32.2 HRC). This behavior is typical of bainitic and martensitic structures, confirming the existence of heterogeneity in mechanical properties produced by chemical segregation. The increase in hardness in the fracture zone may be attributable to the effect of plastic deformation on this property.

CONCLUSIONS

- The fracture failure of the pendant belonging to the endless screw conveyor manufactured from AISI 4340 steel is caused by the formation of concentric circular marks with beach marks in fatigue fracture, indicative of fracture by a cleavage mechanism.
- The fracture in AISI 4340 steel could originate from embrittlement at one of the heat treatment stages associated with the formation of manganese sulfide; this phenomenon usually affects low-alloy steels quenched to martensite and subsequently tempered in the temperature range of 250 °C to 350 °C.

REFERENCES

Albarbar, A. (2013). An investigation into diesel engine air-borne acoustics using continuous wavelet transforms. *Journal of Mechanical Science and Technology*, (27).

Ayatollahi, M., Razavi, S., Chamani, H. (2014). Fatigue life extension by crack repair using stop-hole technique under pure mode-I and pure mode-II loading conditions. *Procedia Engineering*, 74, 18-21.

Cavalieri, F., Luengo, C., Cardona, A. (2011). Análisis de fatiga en muy alto número de ciclos. *Revista Iberoamericana de Ingeniería Mecánica*, 15(1), 03-12.

Gainza-Legrá, A. (2016). *Análisis de rotura del espárrago situado en el cárter de los motores MAN de la unidad empresarial de base generación motores FUEL-OIL de Moa*. (Tesis de Ingeniero Mecánico, Universidad de Moa).

Govindu, N., Jayanand, T., & Venkadesh, S. (2015). Design and optimization of screwed fasteners to reduce stress concentration factor. *J. Appl. Mech. Eng*, 4, 1000171.

Guerra-Fernández, Y., Ordoñez-Hernández, U., González-Fernández, V. (2019). Análisis de la falla de pernos de fijación de las zapatas polares de un motogenerador. *Ingeniería Mecánica*, 22(3), 156-160.

Inzana, J., Varga, P., Windolf, M. (2016). Implicit modelling of screw threads for efficient finite element analysis of complex bone-implant systems. *Journal of Biomechanics*, 49(9), 1836-1844.

Jaramillo, H., & Bacca, L. (2009). Una propuesta para la determinación de la tenacidad a la fractura mediante elementos finitos. *Suplemento de la Revista Latinoamericana de Metalurgia y Materiales*, S1(4), 1641-1616.

Lee, C. H., Kim, B. J., & Han, S. Y. (2014). Mechanism for reducing stress concentrations in bolt-nut connectors. *International journal of precision engineering and manufacturing*, 15, 1337-1343.

Madenci, E., Guven, I. (2015). *The Finite Element Method and Applications in Engineering Using ANSYS*. Second Edition, Springer.

Mantwatkar, A., Chavan, S. (2016). Failure analysis of high tensile industrial fasteners. *International Journal of Scientific and Research Publications*, 6(3), 132-37.

Megias, R., Belda, R., Vercher-Martínez, A., Giner, E. (2023). Estudio de la fractura a compresión de hueso trabecular sano, osteoporótico y artrósico procedente de cabezas femorales humanas. *Revista Española de Mecánica de Fractura*, (5), 21-26.

Srivastava, A., Ponson, L., Osovski, S., Bouchaud, E., Tvrgaard, V., Ravi-Chandar, K., Needleman, A. (2015). The effect of loading rate on ductile fracture toughness and fracture surface roughness. *Journal of Mechanics and Physics of Solids*, 76(7), 20-46.

Vázquez, A., Mantic, V., Muñoz-Reja, M., Távara, L. (2023). Nuevo elemento finito para singularidades logarítmicas de tensión en grietas de interfase tipo Winkler en modo III. *Revista española de mecánica de la fractura*, (5), 213-218.

Additional Information

Conflict of Interest

The authors declare that there are no conflicts of interest.

Author´s Contribution

LRB: Conception of the research. Preparation of samples and data collection. Drafting of the article manuscript, critical revision of its content, writing and approval of the final work. **DGT:** Conception of the research. Preparation of samples and data collection. Worked on the analysis and interpretation of microstructures and on the drafting of the article manuscript, as well as on the critical revision of its content, writing and approval of the final work.

ORCID

LRB: https://orcid.org/0009-0009-1791-0071
DGT: https://orcid.org/0009-0005-3798-2786

Recived: 03/11/2024
Accepted: 28/02/2025